Analysis of skin-stringer debonding in composite panels through a two-way global-local method

Margarita Akterskaia[a,*], Eelco Jansen[a], Stephen Hallett[b], Paul Weaver[b], Raimund Rolfes[a]

[a] *Institute of Structural Analysis, Leibniz Universität Hannover, Appelstr. 9A, 30167 Hannover, Germany*
[b] *Advanced Composites Centre for Innovation and Science, (ACCIS), University of Bristol, Bristol, BS8 1TR, UK*

Abstract

According to various experimental results, stiffened panels under compressive loading are prone to debonding between the skin and the flange of the stringer. In this paper, a novel two-way global-local coupling approach is presented that is able to model progressive separation of the skin and stringer in stiffened CFRP panels under compression. The main goal of this methodology is to examine skin-stringer debonding at two levels of accuracy, taking advantage of the fast calculations at the global level and assessing in detail the damage propagation at the local level. First, critical areas are defined in a global model with a standard mesh, and local models with a considerably finer mesh are created by means of a submodeling technique. Secondly, a local model analysis is conducted, in which cohesive elements are applied to simulate debonding. Particularly important is the appropriate information exchange in both directions between the different steps of the coupling analysis. Averaged degraded properties are defined at the local model level and transferred back to the global level. The applied compressive load is increased and induces a progression in skin-stringer separation. The global-local coupling loops are repeated until panel failure occurs. The approach is applied to a case of a representative one-stringer stiffened panel and to a stiffened panel for which test results are available. A

*Corresponding author
Email address: m.akterskaia@isd.uni-hannover.de (Margarita Akterskaia)

good correspondence with reference results and test results demonstrates the effectiveness of the global-local approach presented.

Keywords: Composite structures, Stiffened panels, Progressive failure analysis, Multiscale analysis, Global-local method, Postbuckling, Skin-stringer debonding, Delamination

1. Introduction

Fiber-reinforced composites and in particular laminated stiffened composite panels are widely used in aircraft design. The reason of the extensive use of composite structures is their remarkable material properties, such as high strength and stiffness to weight ratio. The desire to exploit the advantages of thin, panel-type structures results in post-buckled designs, which make use of the load carrying capability of stiffened panels in the post-buckling regime [1]. For this reason, an efficient and reliable progressive failure analysis method is required in order to examine the damage response, such as damage initiation and evolution, and to determine the final failure load. One of the common failure modes of laminated composite panels is skin-stringer debonding due to relatively low interface strengths. In the current work, the separation between skin and stiffener foot is modelled and investigated by means of a two-way global-local loose coupling approach.

1.1. Debonding and delamination modelling

Delamination and skin-stringer separation in particular is one of the main failure mechanisms of laminated composite structures, together with fibre fracture and matrix cracking. The reason for delamination initiation and propagation is the relatively small interlaminar strength of adjacent plies. Delamination can take place under various combinations of loads and leads to a significant reduction of the load-carrying capacity of the structure. Delamination is commonly modelled numerically by the Virtual Crack Closure Technique (VCCT) or by means of cohesive interface elements.

The VCCT is based on fracture mechanics and the assumption of Irwin that the energy released during the crack extension is equal to the work required to close this crack back to its original length. For the details refer to [2] and [3]. The main drawback of the VCCT is that the crack initiation zone, which could be difficult to predict in case of large and complex structures, should be known in advance.

Cohesive Zone Modelling (CZM) is another approach based on an assumption for the softening region in front of the crack front, that is kept together by the tractions. This idea goes back to Dugdale [4] and Barenblatt [5]. The method of Hillerborg [6] lies at the origin of cohesive elements, considering both crack growth and predicting the crack initiation, which occurs when the tensile stress at the crack tip reaches the tensile strength.

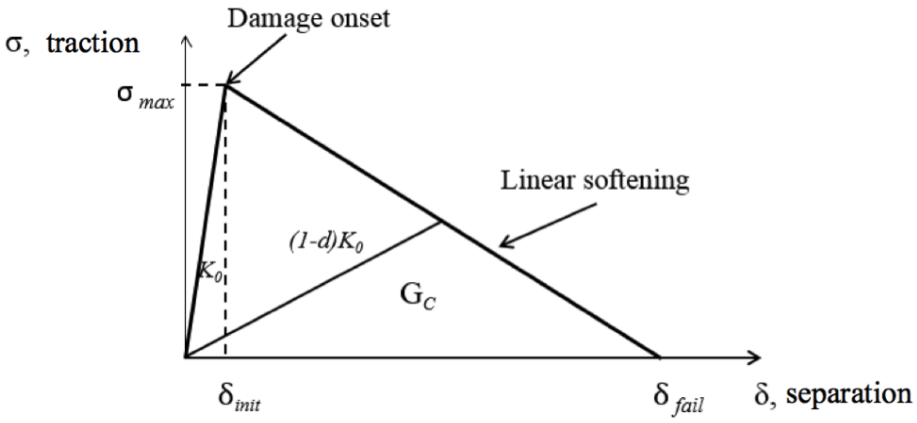

Figure 1: Bilinear traction-separation law.

Interface elements based on the CZM rely on the traction-separation law that is formulated in terms of the traction versus displacement jumps at the interface of potential crack. The most common assumption is that initially linear behaviour until the stress reaches tensile strength σ_{max} for pure mode loading is followed by the softening region until the final separation of the crack surfaces, see Fig. 1. Different shapes of the degradation curve have been proposed in

literature - linear, exponential or trapezoidal [7]. In the present studies, the initial stiffness has been chosen equal to 10^6 N/mm following recommendation of Davila et al. [7]. However, it should be mentioned that some authors prefer to define stiffness value based on material properties and parameters, see Turon et al. [8], for example.

The Cohesive Zone Model was implemented by many authors most commonly in a continuum form (CCZM) where the process zone ahead of a crack tip is modelled with continuum type interface elements. The continuum approach was examined, discussed and improved by Allix and Ladeveze [9], Jiang et al. [10], Turon et al. [11], Camanho and Davila [12] and others. However, convergence difficulties and mesh sensitivity of cohesive elements based on CCZM reflect in the high number of cohesive elements required and result in high computational time. Alternative approach is to apply point-wise discrete elements or Discrete Cohesive Zone Model (DCZM). Borg et al.[13] formulated a discrete cohesive crack model postulating the existence of maximum load surface of adhesive forces. The method was realized by connecting the coincident nodes at the interface and a force-displacement relation was defined for these node pairs. Adhesive forces were reduced following the calculations of the dissipated work until zero value based on the fracture energy criterion. Good agreement with experimental results for mode I, mode II and mixed mode loading was demonstrated. Wisnom and Chang [14] introduced a nonlinear plastic spring as an interface element to examine delamination between the plies of notched composite test models. Xie and Waas [15] applied the DCZM based on non-linear spring type elements and traction-separation bilinear cohesive law for three fracture tests. On given examples, this technique was shown to be insensitive to mesh density or load increment and no convergence difficulties were encountered. Hallett and Wisnom [16] performed modelling of damage in tension for notched laminates by employing interface elements based on three-degree-of-freedom non-linear springs. Comparison with tests proved the model to be accurate enough until occurrence of fibre failure. Jiang et al. [10] proposed a constitutive law for cohesive interface areas for mixed-mode delamination process. Application was

performed on scaled open hole tension tests with a non-linear spring element for the interface modelling. These discussed discrete techniques for the simulation of adhesive behaviour require accurate calculation of forces or stresses which for relatively complex structures could be achieved only with a high computational cost. Therefore, various multi-scale approaches could be utilized to minimize the number of constitutive equations on the one hand, and to obtain reliable results on the other hand.

1.2. Skin-stringer separation in stiffened panels

Skin-stringer separation in composite stiffened panels was considered in many analytical and numerical investigations with the aim of examining their progressive damage, buckling and post-buckling behaviour. In the following, only a few of them will be mentioned. Wang and Bigger [17] studied the stresses between skin and stiffener of composite panels with specific attention on separation between them. Balzani and Wagner [18] examined debonding between skin and stiffner in stiffened panel with cohesive elements. Raimondo and Riccio [19],[20] performed skin-stringer debonding analysis on the test case of two single stringer panels by means of improved VCCT. Yap et al.[21] examined skin-stringer debonding of curved T-stringer panels. A stiffened panel was modelled with shell elements and rigid bars were utilized to tie skin and stringer with debonding being modelled based on fracture mechanics. Falzon et al.[22] presented experimental results for three stiffened panels under compression investigating crack propagation through the skin-stiffener interface.

1.3. Global-local methods for skin-stringer separation of stiffened panels

Global-local methods are indispensable design tools that gained their recognition for modelling of large and complex structures because of the need to reduce computational effort on the one hand, without losing knowledge about the critical areas prone to damage on the other hand. Skin-stringer separation in laminated panels was observed during numerous experiments [1] and various global-local approaches were suggested and implemented through finite element

analyses. Some definitions of coupling global-local methods have been proposed in [23] proposing to distinguish between loose and tight procedures as well as between one-way and two-way approaches. Tight procedure means that global and local models are connected and calculated simultaneously, whereas during the loose coupling analysis both global and local models are treated consecutively. The latter methodology requires the separate creation of local models and could offer great flexibility concerning their size and location which could be adjusted along the analysis. Loose coupling technique can be subdivided in one-way and two-way approaches. The difference between one-way and two-way techniques consists in the direction of the information exchange between the levels. Regarding the one-way coupling method, information is transferred only in one direction. This commonly means, that progressive failure analysis could not be performed because the information regarding the damage state is transferred only once. However, this could be also helpful when the damage location is known a priori and failure only needs to be investigated at the local level. In more complicated cases when the damage area is not known and might expand when increasing the load, the two-way coupling approach is recommended to overcome aforementioned limitations.

According to the proposed distinction, the term tight coupling could be applied to following works. Krueger et al. [24] analysed a three-stringer panel with embedded debonding under shear loading. The area of probable debonding evolution was accurately modelled with solid elements, whereas the shell elements with a coarser mesh were applied to the whole model. VCCT was implemented to model debonding. Borrelli et al.[25] examined two coupling methods: point-wise kinematic coupling and weighted residual coupling to perform tight global-local analysis of initially delaminated stiffened panel. Shell elements and a coarse mesh were used for the global area, whereas the local area surrounding delamination was modelled with solid elements and a finer mesh. Modified virtual crack closure technique (MVCCT) was used to model delamination. The results were compared to the reference model with solid elements. Alesi et al. [26] presented a global-local method based on coupling with

multipoint constraints.

One-way coupling includes mainly methods of the information transfer realized in the global-local direction. Faggiani and Falzon [27] conducted an optimization procedure for a stiffened composite panel through improving damage resistance of the skin-stringer interface by means of a genetic algorithm. The global-local method using a submodeling technique was applied. Bertolini et al.[28] presented a global-local one-way coupling approach to model skin-stringer debonding by means of VCCT technique. The method was applied to a one-stringer T-shape panel subjected to seven-point bending. Ultimately, two large stiffened panels with Omega-stringers under compressive and shear loading were examined. Shell and solid elements were utilized to create global and local models respectively. Reinoso et al.[29] applied a one-way global-local procedure to evaluate the computational analysis and experimental results for the stringer runout effect in a composite panel. Two approaches were compared in Abaqus: submodeling technique and shell-to-solid coupling. Vescovini et al. [30] proposed one-way global-local analysis for the Omega-shaped multi-stringer panel loaded in compression. Both global and local models were composed of shell elements. Cohesive elements were applied between skin and stringer in the local models allowing for determination of delamination onset and growth. Local models created by means of submodeling procedure had a pre-determined size and local analysis was performed five times moving the local model along the stringer.

Orifici et al. [31] proposed a global-local methodology that could be regarded as two-way coupling for the detection of the ply damage and skin-stringer separation in the postbuckling regime of stiffened panels. After the coarse analysis of the global model, the obtained displacements were used as boundary conditions for local models with a finer mesh. Delamination onset was predicted at the local level where 3D stresses are calculated accurately. VCCT was applied to simulate debonding propagation at the global level. Bettinotti et al. [32] suggested a substitution method for the multiscale analysis of delamination under high-velocity impact that allows concurrent run of global and local anal-

ysis. A comparison was performed with tie constraint between different regions and submodeling approach. The approach was based on the separate code and integration of this algorithm to an Abaqus/Explicit was carried out.

1.4. Objectives

A two-way loose coupling approach was developed earlier to simulate the post-buckling progressive failure behaviour of a panel-type structure with intralaminar damage in an efficient way [23], [33]. In these earlier works, the global-local approach has been validated for typical test cases of a panel with one stringer and two stringers. Panels without any initial defects were considered as well as pre-damaged panels. Satisfactory agreement with numerical and experimental reference results demonstrated the potential of this coupling method. Recently, application of the approach to a larger panel with five stringers was conducted to illustrate the main advantages of this method [33].

The aim of the present work concerns the development of a new global-local coupling approach that enables the numerical simulation of the initiation and propagation of skin-stringer separation. Moreover, a novel procedure is elaborated in order to enable the information transfer from local to global level to overcome the limitations of the aforementioned techniques. This comprises simulation of the damage propagation at the global level by means of accounting for the stiffness degradation from the local level which is not possible within one-way approaches. High flexibility concerning creation, extension and unification of local models during damage evolution is advantageous compared to tight coupling techniques. The developed global-local method can be easily implemented in general-purpose finite element programs.

2. Analysis Methodology

The two-way loose coupling procedure for modelling skin-stringer separation of a stiffened panel is described below in details. The procedure starts with a global analysis with shell elements and relatively coarse mesh density that is

carried out in order to determine critical damage areas. Opposite nodes of skin and stringer are tied in the interface area by spring type connector elements with linear elastic behaviour. The stiffness of particular connector elements along the solution process should be updated and so represent the degradation part of the traction-separation law. Hence, discrete cohesive behaviour is chosen for the global level. Cartesian-type connector elements in Abaqus satisfy these requirements. Initial stiffness of interface elements is specified based on the following relation:

$$K = \frac{EA}{t} \tag{1}$$

where E is the Young's modulus of an adhesive layer, A and t are in-plane nodal area and thickness in the normal direction of the adhesive element respectively.

Estimation of the critical areas prone to delamination is performed through an additional Python script for connector elements based on the quadratic stress criterion the same as for cohesive elements, see Eq. 3. Normal and shear stresses at the nodes of connector elements are calculated accounting for the free edge and internal nodal areas that are tied by connector elements:

$$\sigma_{i3} = \frac{F_i}{A_{el}}, \quad i = \overline{1,3} \tag{2}$$

where F_i is a nodal force, A_{el} determines a nodal area of applied force and here represented as a sum of one quarter of each element area tied to that node. Therefore, A_{el} either represents the full in-plane area of the shell element A_{int}, referring to Fig. 2 for interior connectors, or a half of this area denoted as A_{ext} corresponding to the case when connectors tie the edges. Index i specifies local Cartesian directions. σ_{33} corresponds to the normal stress that acts through the thickness, σ_{13} and σ_{23} are two in-plane shear stresses. In Eq. 1 the penalty stiffness definition includes non-material parameters such as nodal area A and thickness t. The force F_i from Eq. 2 is proportional to the corresponding stiffness which means that the stresses σ_{i3} are independent from the nodal area and depend only on the thickness of the adhesive layer. Connector elements that tie conventional 2D shell elements of skin and stringer are demonstrated in

Fig. 2. Different nodal areas A_{ext} and A_{int} described earlier are shown in this figure.

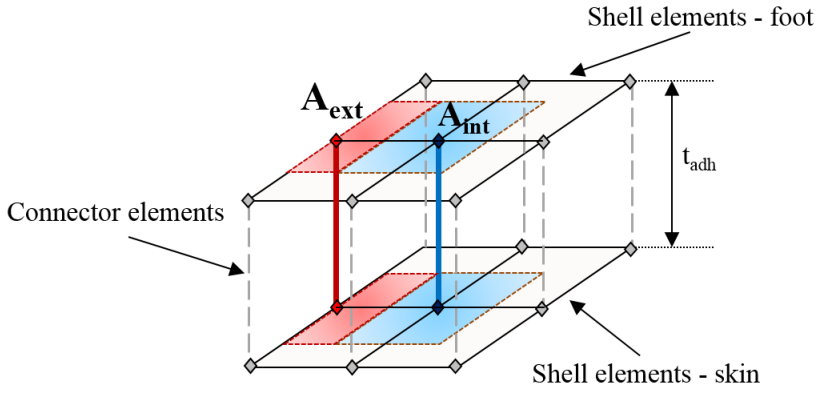

Figure 2: Discrete interface elements connecting skin and stringer represented by shell elements.

Afterwards, the critical areas are examined during the next step - local analysis where separate local models are created. Solid elements are utilized to model the skin and the stringer and cohesive elements for the interface area between them. Fine mesh discretization is used for these local models. Nodal displacements from the global model are transferred to the selected boundary nodes of the local model as kinematic constraints by the means of the Abaqus shell-to-solid submodeling procedure [34].

The quadratic stress criterion is chosen to predict initiation of debonding in the local model:

$$\left(\frac{<\sigma_n>}{N_{max}}\right)^2 + \left(\frac{\sigma_s}{S_{max}}\right)^2 + \left(\frac{\sigma_t}{T_{max}}\right)^2 = 1 \tag{3}$$

Here $< \ldots >$ represents McCauley brackets operator used here to recognise that compression is generally not involved in interface separation. σ_n is a stress in the normal through-thickness direction, σ_s and σ_t are nominal stresses acting in the first and second shear directions and N_{max}, S_{max}, T_{max} are the corresponding strengths.

Delamination propagation under mixed-mode loading could be traced by means of the Benzeggagh and Kenane criterion [35] extended to three dimensional case:

$$G_c = G_{IC} + (G_{IIc} - G_{IC}) \left(\frac{G_{II} + G_{III}}{G_I + G_{II} + G_{III}} \right)^{\eta} \tag{4}$$

where G_{IC} and G_{IIC} are mode I and II fracture toughness and G_I, G_{II}, G_{III} are single mode energy release rates corresponding to fracture modes I, II and III and their sum is the total energy release rate. The parameter η is determined empirically, assumed to be 2.284 in the current studies [8].

A scalar damage variable d is utilized to identify the damage state. It varies from 0 when there is no damage to 1 when the interface connection is fully failed. Camanho and Davila[12] suggested the following damage variable for monotonic loading:

$$d = \frac{\delta_{fail}(\delta - \delta_{init})}{\delta(\delta_{fail} - \delta_{init})} \tag{5}$$

where d is the damage variable, δ is the current maximum relative displacement, δ_{init} corresponds to the displacement of the delamination beginning and δ_{fail} is the displacement of the complete failure.

The stiffness of the cohesive element used in linear traction-separation law is defined following Camanho and Davila [12]:

$$K = \begin{cases} K_0 & \delta < \delta_{init} \\ (1-d)K_0 & \delta_{init} < \delta < \delta_{fail} \\ 0 & \delta > \delta_{fail} \end{cases} \tag{6}$$

where K_0 is the initial penalty stiffness that is degraded after displacement δ reaches the value of δ_{init} and becomes 0 when the crack opening is equal to δ_{fail}.

During the postprocessing phase, that follows the local model analysis, damage variable d that defines the degradation stage of each particular cohesive element is extracted in order to calculate the decreased stiffness of an appropriate connector element. According to the global-local approach discussed before,

mesh densities at global and local levels do not correspond to each other. In order to overcome this difference and to transfer degraded stiffnesses of each interface element from the local to the global level, a special averaging technique should be applied. First of all, an averaged local stiffness is calculated for each area that corresponds to one connector element:

$$K_{local} = \frac{\sum_{i=1}^{N} K_{local,i}}{N} = \frac{\sum_{i=1}^{N} (1 - d_i) K_{local,0}}{N} = K_{local,0} \left(1 - \frac{\sum_{i=1}^{N} d_i}{N} \right) \quad (7)$$

where $K_{local,0}$ is the initial stiffness of a cohesive element, i denotes one of N local cohesive elements and d_i is the corresponding damage variable. Hence, to obtain an averaged local stiffness that conforms to one connector element at the global level, initial stiffness should be multiplied by the coefficient that stems from the averaged value of damage variables. This multiplication factor is utilized to obtain degraded stiffness of each particular connector element at the global level and ensure transfer of information of the damaged state from local to global level.

With new reduced global properties for connector elements, the global analysis is performed again applying initial stiffness in the interface area until the increment when the damage was predicted. Starting at that increment new degraded properties are utilized for each connector element. These coupling steps are repeated until convergence in reaction forces in the direction of the applied load is reached. In our case, the reaction force from global analysis is also compared to the reaction force of the reference solid model.

The flowchart of the two-way coupling procedure for the skin-stringer debonding along with information exchange between global and local levels of analyses is presented in Fig. 3.

Hence, the coupling loop consists of three major operations that are repeated iteratively at two levels of accuracy until the final collapse is determined:

1. Global analysis to evaluate the areas of a probable damage and to define local models geometry.

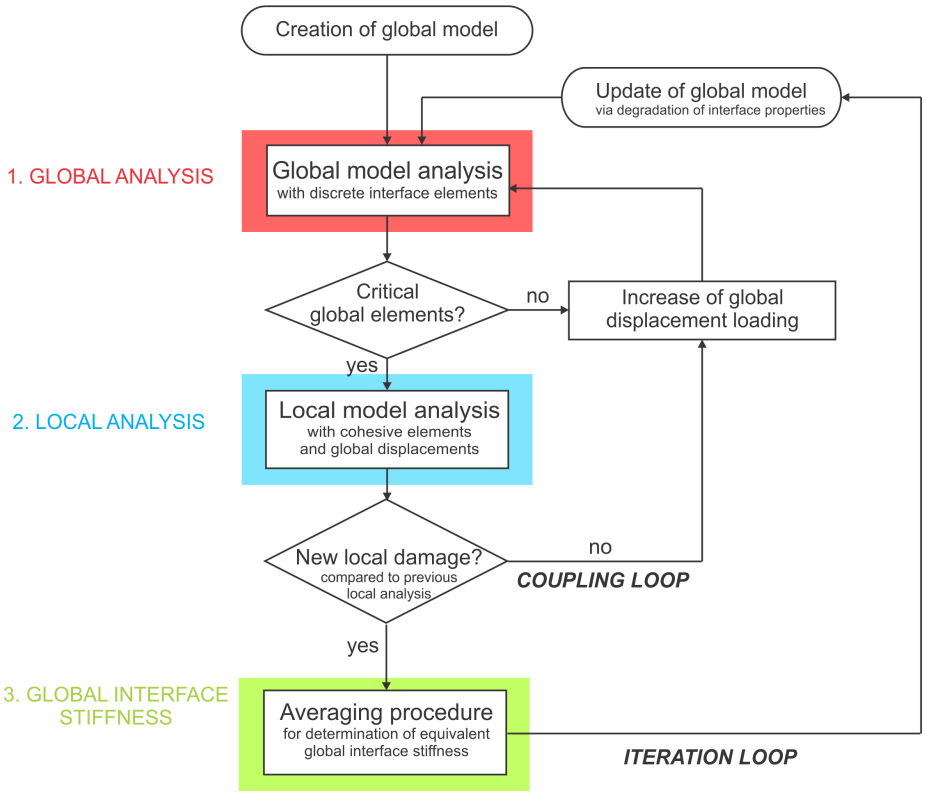

Figure 3: Flowchart of the two-way loose coupling procedure for the skin-stringer debonding.

2. Local models obtain displacements as boundary conditions from the global solution. After carrying out numerical calculations for local models, damage variables for each cohesive element are obtained.
3. Global interface stiffness is calculated based on average damage variables and transferred back to the global level.

The main steps of this global-local method are illustrated on a Fig.4 for an example of a one-stringer panel: global analysis, local analysis, and adhesive properties averaging. These three steps are repeated consecutively until the final collapse is detected. The information exchange between global and local level that ensures two-way coupling is performed at each stage.

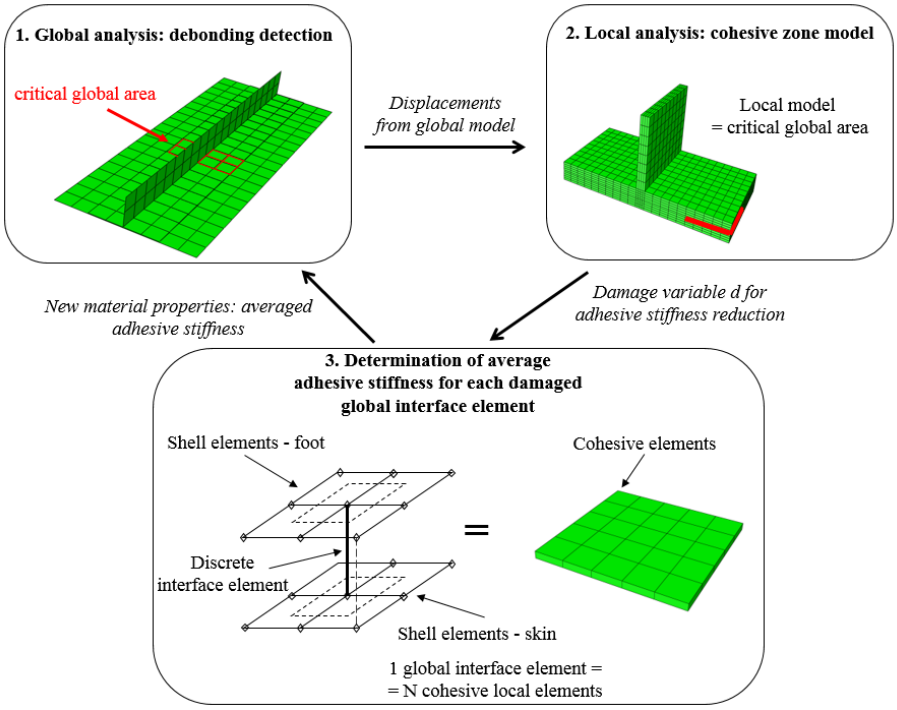

Figure 4: Two-way loose coupling procedure for the debonding: application to a composite stiffened panel.

3. One-stringer stiffened panel under compression

In this section, a stiffened composite panel with one T-stringer under compression, see Fig. 5, is analysed in order to capture skin-stringer debonding with the global-local approach. The unidirectional symmetrical layups for the skin and the stringer are chosen as $[0, 90]_s$. One of the transverse edges is fully clamped, except for the longitudinal direction, and displacement is applied at the opposite edge. Both longitudinal edges are free to deform. Material and geometrical parameters are listed in Tables 1 and 2 respectively. These values were taken from the academic application suggested by [23].

Table 1: Geometry of stiffened composite panel.

Description	**Value**
Panel length, l (mm)	100
Panel width, w (mm)	40
Stringer width, b (mm)	20
Stringer height, h (mm)	8
Laminate thickness, t_{skin}, t_{blade} (mm)	1
Adhesive thickness, t_{adh} (mm)	0.2

Table 2: Material data for composite and adhesive.

Stiffness properties	**Value**
Young's modulus in 1-direction, E_{11} (GPa)	146.5
Young's modulus in 2-direction, E_{22} (GPa)	9.7
Shear modulus in 12-plane, G_{12} (GPa)	5.1
Poisson's ratio, ν_{12}	0.28
Young's modulus of adhesive, E_{glue} (GPa)	3.0
Poisson's ratio of adhesive ν_{glue}	0.4

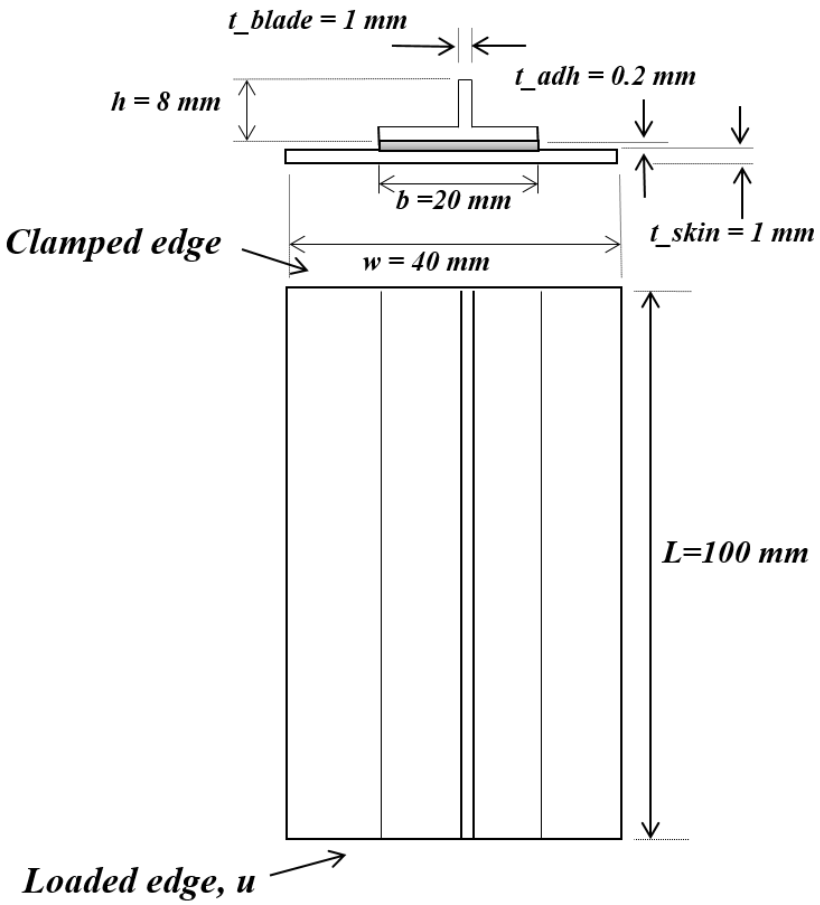

Figure 5: Geometry of stiffened panel.

3.1. Global model: linear elasticity

The global model, which is referred to a model with a coarse mesh from first global step consists of 280 conventional 4-node shell elements with reduced integration (S4R in Abaqus) and a side-length of 5 mm, which are used to represent the skin and the stringer. As discussed earlier, the adhesive layer is not modelled with cohesive elements in order to keep the global model analysis fast and consistent. Instead of cohesive elements, 105 connector elements of Cartesian type (CONN3D2 in Abaqus) are applied. The *Offset parameter is implemented to reference shell surfaces that offsets the nodes of stringer

and skin from the middle surfaces towards the lower and upper surfaces respectively. This technique facilitates the implementation of a connection between

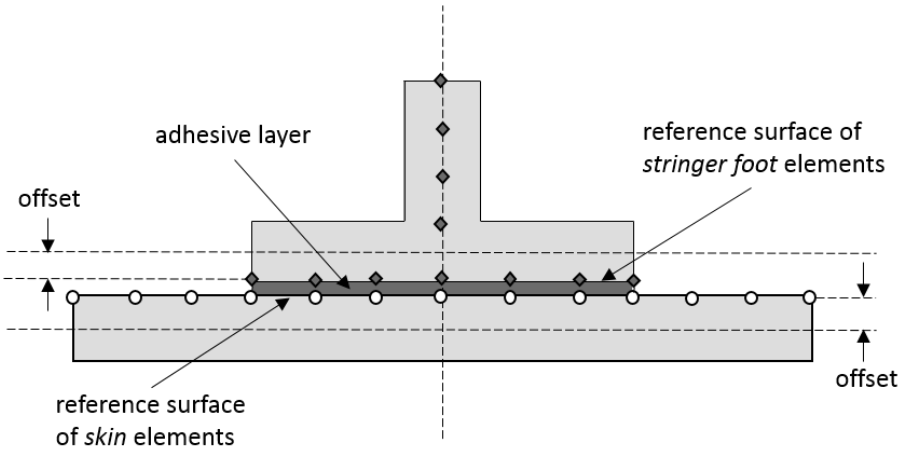

Figure 6: Geometry of section of stiffened panel.

shell nodes of skin and stringer and also ensures that real lengths and nodal forces are calculated for interface elements. Mesh density is the same for the full structure and corresponding nodes of skin and stringer are situated in front of each other, as shown in Fig. 6, so that they could be easily tied by connector elements. Critical areas, where the onset of skin-stringer separation is expected, are detected relying on the quadratic stress criterion given in Eq. 3. Buckling is triggered by utilizing an initial geometrical imperfection as the first eigenmode of the preliminary linear buckling simulation of the stiffened panel. However, as skin and stringer are tied by connector elements, the consequent degradation of the interface stiffnesses may lead to the problem concerning layer interpenetration. To avoid this issue, a *Clearance option available in Abaqus is utilized. An initial clearance of 0.00005 mm is specified to prevent node penetration of two shell surfaces. After completion of the local analysis, degraded stiffnesses of connector elements are calculted based on Eq. 7, multiplying global connector stiffness by the corresponding averaged damage variable from local cohesive elements. Then global analysis is performed from the beginning. Connector el-

ements retain initial properties until the loading displacement is reached when the damage onset was predicted. Afterwards, each connector element obtains degraded or not degraded stiffness based on local analysis information. All the stiffnesses are collected and read from the separate input file.

3.2. Local models: nonlinear material model

Locations of local models are identified based on critical areas determined during the global analysis. Local models represent skin and flange of the stringer where the debonding is expected to propagate. The web of the stringer is also included in the local model, as further investigations should be conducted to understand the influence of the stringer on the debonding mechanism. The skin and the stringer are modelled with 8-nodes linear solid elements (C3D8 in Abaqus) and 8-nodes cohesive elements with non-zero thickness (COH3D8 in Abaqus) and bilinear traction-separation law are chosen for the adhesive layer. Interface properties, such as strength and fracture toughness, are summarised in Table 3. The in-plane length of the local element is 1 mm as with preliminary mesh convergence studies it was confirmed to be sufficiently enough for this kind of panel. The out-of-plane length is 0.25 mm which leads to one element per lamina in thickness direction. Four cohesive elements per length of one local element are utilized, as mesh convergence verification has not determined significant improvements with further increase of the cohesive elements number, see Fig. 7. To connect solid elements of skin and foot of the stringer to the larger number of cohesive elements, *Tie constraint is utilized. Following the advice in [29], the master surface belongs to solid elements, whereas slave surfaces are defined on the cohesive elements. During the softening behaviour and stiffness degradation that is characteristic for cohesive elements convergence difficulties may occur in Abaqus Standard. That is the reason for using viscous regularization of the constitutive equations to overcome this issue. A relatively high viscous parameter of 10^{-3} has been chosen for the local analysis with cohesive elements. Though each particular case requires a special judgement in order to keep a balance between numerical convergence and experimental results, as

higher viscosity parameters might result in higher load peaks.

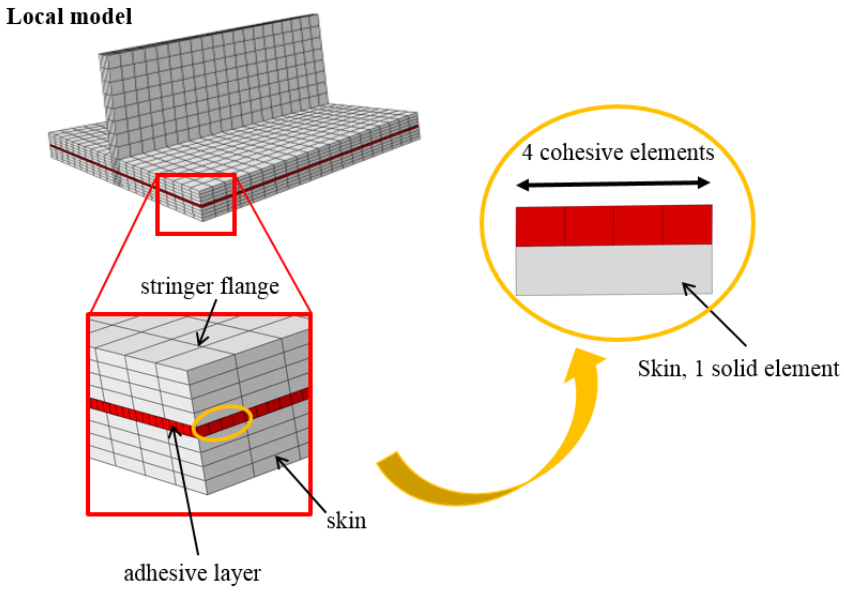

Figure 7: 3D local model with cohesive elements.

After local numerical analysis is terminated, the degraded damage variables d, described in Eq. 5 are extracted for each local cohesive element with the help of an additionally Python written script. The procedure is similar to the extraction of local damaged intralaminar properties conducted in previous studies [23].

3.3. Local-global transition

The difference in mesh size between the global and local model requires the implementation of an averaging procedure, see Eq. 7, to determine the equivalent reduced global stiffness of interface elements. Afterwards, a mapping technique is applied to map each global connector element to the area of local cohesive elements and thereby the degraded stiffness of this connector element is determined. This is realized in a Matlab procedure using the coordinates of the elements.

Table 3: Material data for cohesive elements.

Cohesive element properties	**Value**
Interface element stiffness before the damage onset, K (N/mm^3)	10^6
Interfacial strength, mode I, τ_I (MPa)	61
Interfacial strength, mode II and III, τ_{II}, τ_{III} (MPa)	68
Fracture toughness, mode I, G_{Ic} (N/mm)	0.243
Fracture toughness, mode II and III, G_{IIc}, G_{IIIc} (N/mm)	0.514

3.4. Reference solid model

The reference model is a full 3D model of a stiffened panel. It consists of 30,400 linear solid elements (C3D8 in Abaqus) for skin and stringer of the panel and 38,400 cohesive interface elements (COH3D8 in Abaqus) for the adhesive layer. The preliminary studies also include a test with implementation of 20-node bilinear solid elements for modelling skin and stringer. No significant improvements regarding damage prediction or final failure load were observed. Hence, it has been concluded that linear solid elements exhibit a satisfactory level of accuracy and efficiency. In order to keep consistency, the mesh density chosen for the reference model is the same as for local models. Also a bilinear traction-separation law is utilized for cohesive elements in order to investigate debonding between skin and stringer. An initial geometrical imperfection is represented by the first eigenmode of the stiffened panel similarly to the global shell model.

3.5. Coupling results

The coupling procedure is carried out through six coupling loops, each of them consists of several iterations. During each coupling loop, the prescribed displacement is increased based on the following principle: either critical area should evolve or new critical regions should appear. This leads to a consequent expansion of the local models. Fig. 8 demonstrates six overlay plots of the

separated global shell and the local solid models where increase of the local models could be distinguished from step 1 to step 2 and from step 3 to step 4. It should be mentioned that connector elements demonstrated an evolution of the damage during some coupling loops in the areas of already existing local models. In these cases, local analysis was conducted with the same size of the local model as for the previous coupling loop, as no extension of the local model would be justified.

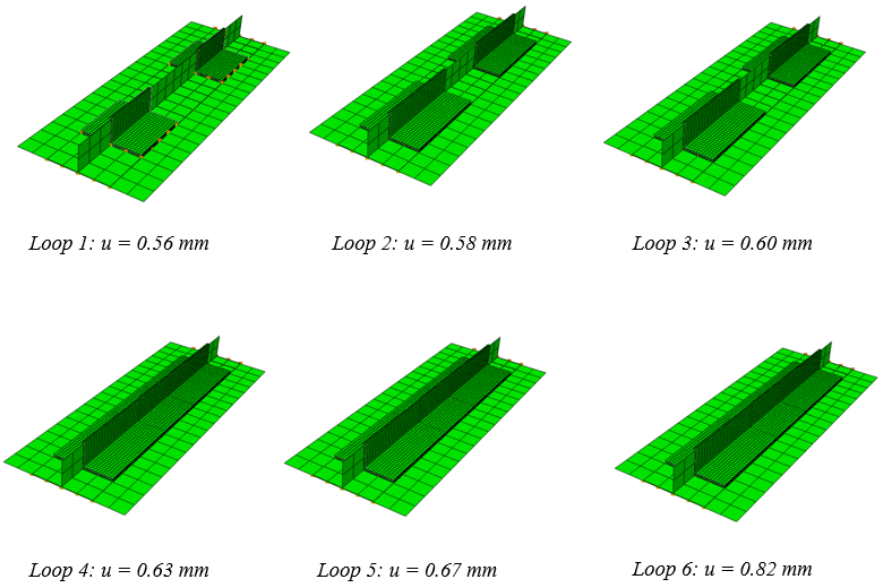

Figure 8: Overlay plots of stiffened panel of global and local models from coupling loops 1-6.

The damage evolution in connector elements in the global model for six coupling loops is illustrated in Fig. 9. During the simulation process the first area of probable skin-stringer separation is detected by the quadratic stress criterion, see Eq. 3, at the prescribed displacement of 0.56 mm. At this applied displacement, damage takes place at free edges on both longitudinal sides of the panel, see Fig. 10a. Two local models are created for these critical regions. The coupling loop is repeated until the convergence at the global level is reached. The skin-stringer debonding onset predicted at the global level is confirmed by the

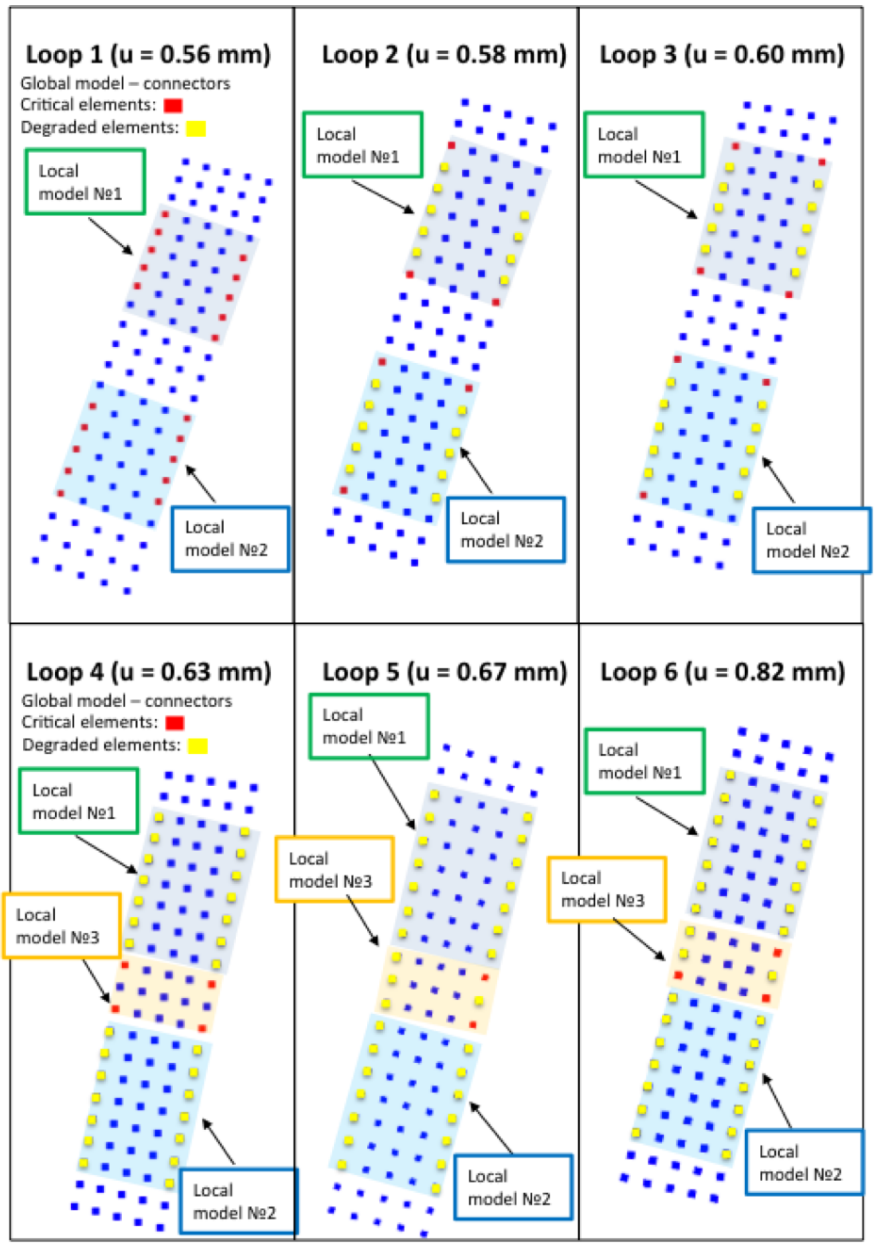

Figure 9: Coupling loops 1-6. Debonding propagation in the global model.

local analysis results, as both local models show cohesive elements degradation at the free edges, see Fig. 10b. Updated reduced stiffnesses for the interface

elements are calculated and transferred back to the global model enabling the connection of different model levels.

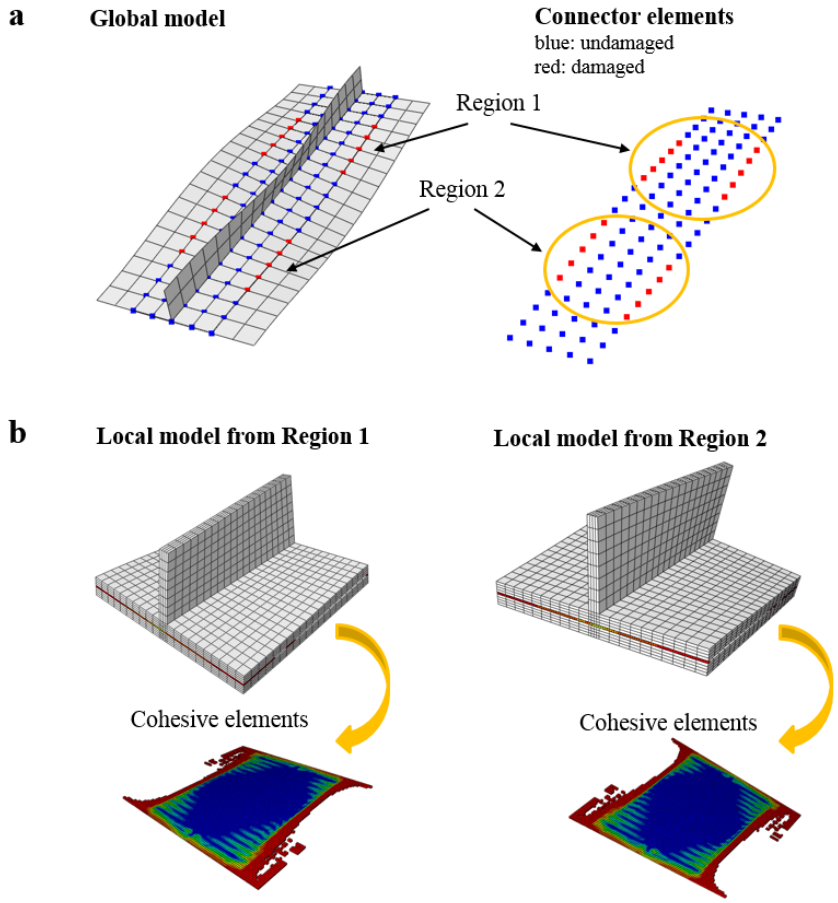

Figure 10: Coupling loop 1. (a) Critical global regions of interface elements related to skin-stringer separation, (b) local models for the Regions 1 and 2 with corresponding damaged cohesive elements.

Along the second coupling loop with displacement of 0.60 mm damaged areas are enlarged as new connector elements are identified as being critical, see Fig. 9. It is important to mention that due to the previously degraded stiffness of connector elements the load in the interface has been redistributed to the neighbouring elements. The third coupling loop with an increase of applied displacement to 0.58 mm registers no expansion of local models. After the

completion of the third coupling loop, an increase of displacement to 0.63 mm during the fourth coupling loop provokes the spread of the skin-stringer debonding along both free edges. The third local model has been created in the middle of the panel, refer to a Fig. 8 where three local models have neighbouring elements. The reason for examining three local models instead of single unified one is that this approach is slightly faster and is assumed to be sufficienly accurate. The fifth coupling loop has prescribed displacement of 0.67 mm and demonstrates damage evolution within the sizes of local models identified previously. Finally, in the sixth coupling loop the prescribed displacement reaches 0.82 mm. This final displacement increase results in an rapid propagation of the damage through the interface, followed by almost full deletion of cohesive elements in the local models and in total stiffness reduction of the whole structure. Consequently, the final failure of the stiffened panel is attained which is regarded as the logical end for the coupling procedure.

Global, local and reference models analyses were carried out under the same computational characteristics. Relative calculation times are 330 s for the last global model step and 40,884 s for the full 3D reference model, respectively. This difference is due to the high level of discretization and inclusion of material nonlinearity to the reference model. However, in order to determine computational time of the global-local procedure, global model should be solved several times until the detection of the final failure, and this time should be added to the calculation of the local models. In Table 4 numerical characteristics of aforementioned models are represented. In the current studies, local models under consideration demonstrated computational time from 2,449 s for the first local model at the first coupling loop to 13,339 s for the second local model at the last coupling loop. Hence, for the selected benchmark panel the global-local approach demonstrates a computational time similar to the one of the reference model. The relatively large computational effort of the global-local results can be attributed to the large size of the local models as compared to the global model, see Fig. 8. It can, however, be noticed that the first local model was solved approximately 16 times faster than the full reference model. It is there-

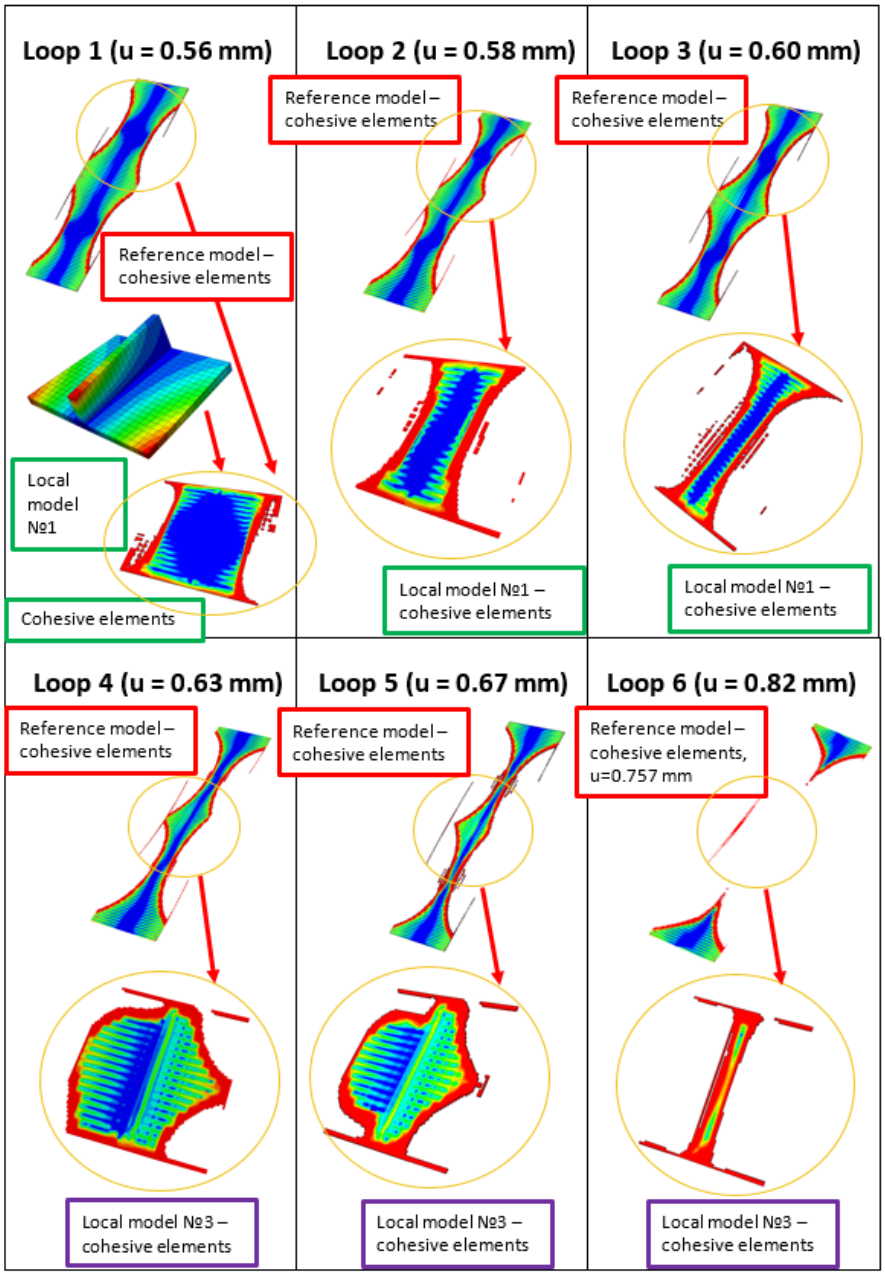

Figure 11: Comparison of reference model with local models results for cohesive elements.

Table 4: Computational characteristics of models.

Model	**Number of nodes**	**Number of elements**	**Degrees of freedom**	**Relative computational time, s**
Reference model	192,136	68,800	463,980	40,884
Global model, 6^{th} coupling loop	756	385	2,331	330
Local model, 1^{st} coupling loop	35,636	12,160	86,160	2,449
Local model, 6^{th} coupling loop	51,816	18,240	126,420	13,339

Table 5: Comparison between debonded area of reference and local models.

Model	**Loop 1**	**Loop 2**	**Loop 3**	**Loop 4**	**Loop 5**	**Loop 6**
Reference model, debonded area, mm^2	199	244	355	151	284	484
Local model, debonded area, mm^2	118	281	477	154	221	425

fore important to note that in case of the localized and relatively small area of damage the global-local method is not only an accurate approach, but also advantageous in time-saving.

A comparison between reference model and local models degradation is shown in Fig. 11 for coupling loops 1 to 6. In Table 5 a comparison between the debonded areas of the local models and the corresponding regions of the reference model is presented for each coupling loop. During the first coupling analysis the local model demonstrates slower deletion of cohesive elements resulting in a difference of 41% in debonded area compared to the reference model, see Table 5. Though already after coupling loop 2, reference and local model results are in a relatively good agreement. During coupling loop 4, damage at free edges in the middle of the panel is detected at the global level. The local model shows degradation in this area, though the damage in the reference model evolves slightly differently. However, in the sixth coupling loop the local model

demonstrates the deletion of almost all distorted cohesive elements with a good agreement to the reference model.

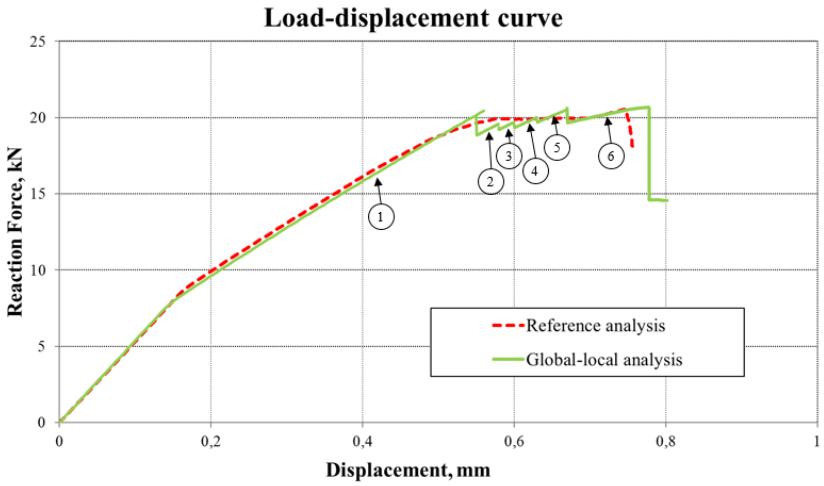

Figure 12: Load-displacement curve for progressive failure analysis of stiffened panel.

Load-displacement curves for both reference solid model and coupling loops are presented in Fig. 12. Distinct drops of the coupling curve correspond to each global-local loop that is characterised by the reduction of interface stiffness. Each coupling loop is enumerated from 1 to 6 on the plot. The reference curve is smoother because the cohesive elements properties have been degraded incrementally. Both curves are in a good agreement, in particular with regard to the structural stiffness before and after first buckling takes place. Buckling in the coupling simulations occurs slightly earlier at a displacement of 0.147 mm and for the reference model at 0.167 mm resulting in a slight difference in curves, though lying in parallel and, thus, having similar stiffnesses. The final failure of the reference model takes place at a displacement of 0.76 mm that corresponds to the load level of 20.54 kN, whereas for the coupling loops the maximum displacement and load are 0.78 mm and 20.68 kN respectively. The relative deviation between maximum supported loads for the stiffened panel in compression is reported to be around 0.7%. The latter conclusion demonstrates the

capability of the global-local approach to simulate full 3D behaviour with regard to a reliable prediction of skin-stringer debonding initiation, evolution and final collapse.

4. Validation with experimental results

In this section, the applicability of the global-local approach to a real stiffened composite panel with available experimental results is investigated. The specimen has been tested by Orifici et al. [31] and denoted as initially debonded single-stiffener D1 panel during their studies. This particular choice of a panel with preliminary skin-stringer separation is explained by the goal to examine a specimen with localized debonding that is expected to dominate over the intralaminar damage and demonstrate the full advantage of creating relatively small local models. In Fig.13 a sketch of geometric configuration for the debonded panel is shown, the geometric and material data of the specimen are reported in Tables 6 and 7 respectively with descriptions used by Orifici et. [31]. The panel was manufactured with IM7/8552 UD material for the skin and stringer, whereas for the adhesive layer FM 300 was utilized. In the previous section the interface properties were taken for this material also from [31], refer to Table 3 for details.

4.1. Global model: linear elasticity

The shell global model is created similarly to the aforementioned benchmark panel. After a preliminary mesh convergence studies, the in-plane size length of 4 mm is determined, which resulted in 2800 conventional shell elements (S4R in Abaqus) and 909 connector elements tying the opposite lying nodes of the skin and stringer surfaces. The first eigenmode is utilized as an initial geometric imperfection to perturb the panel in a postbuckling regime similar to the one described in [31]. The following boundary conditions are applied: (1) one transverse edge is fully restrained denoted as clamped end, (2) the opposite edge is restricted to move in any direction except longitudinal and correspond

Table 6: Geometry of initially debonded stiffened composite panel D1 (from [31]).

Description	**Value**
Total length, L (mm)	400
Free length, L_f (mm)	300
Width, b (mm)	64
Skin lay-up	$[90, \pm 45, 0]_s$
Stiffener lay-up	$[(\pm 45)_3, 0_6]_s$
Ply thickness, t (mm)	0.125
Stiffener height, h (mm)	14
Stiffener width, w (mm)	32
Debond length, d (mm)	80

Table 7: Material data for IM7/8552 carbon/epoxy unidirectional tape (from [31]).

Stiffness properties	**Value**
Young's modulus in 1-direction, E_{11} (GPa)	147
Young's modulus in 2-direction, E_{22} (GPa)	11.8
Shear modulus in 12-plane, G_{12} (GPa)	6
Shear modulus in 31-plane, G_{31} (GPa)	6
Shear modulus in 23-plane, G_{23} (GPa)	4
Poisson's ratio, ν_{12}	0.3

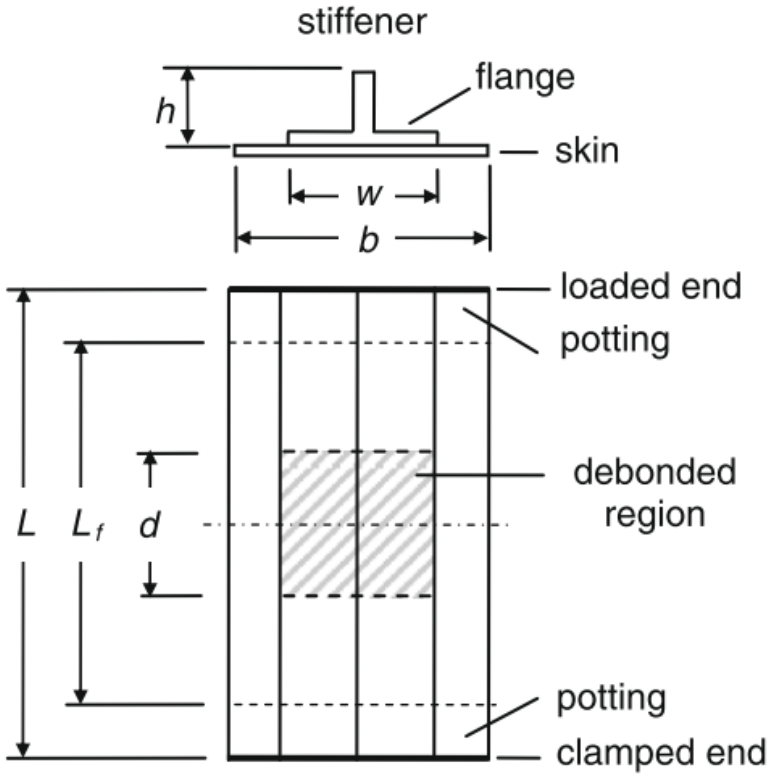

Figure 13: Geometry of initially debonded stiffened panel design D1 (from [31]).

to a loaded end, (3) two pottings are allowed to move only in the longitudinal direction, see Fig. 13. Both longitudinal edges remain free to deform.

4.2. Local models: nonlinear material model

The local models have the same structure as the previous model - 8-nodes linear solid elements (C3D8 in Abaqus) with a side-length of 1 mm and 1 element per lamina in thickness direction resulting in a size of 0.125 mm for the skin and the stringer. Cohesive elements with bilinear traction-separation law represent the interface layer in order to track the beginning and development of the skin-stringer debonding. Four cohesive elements are utilized per in-plane side of a solid local element. The selected discretization repeats the previous model - one element per lamina in the thickness direction with 1-mm in-plane size length

for structural elements. Four cohesive elements per side of one solid element are chosen.

4.3. Coupling results

Global-local analysis has been conducted through four coupling loops with consequent increase of the prescribed displacement up to the following values: 1.0 mm, 1.4 mm and 1.6 mm and 2.0 mm respectively. According to experimental and numerical results, the skin and the foot of the stiffener have buckled in opposite directions that excludes issues with probable initial interpenetration of the layers during the calculations. The onset of skin-stringer separation is predicted based on the stress quadratic criterion (Eq. 3) and begins in the areas of the initial debonding at the applied displacement of around 0.8 mm, see Fig. 14. Two local models are created for these regions respectively to examine the debonding evolution in details, see Fig. 15. A determination of global regions that are prone to debonding is proved by both local analyses demonstrating a damage onset and growth in cohesive elements. It is important to mention that the size of local models is selected appropriately, as they both cover not only distorted cohesive elements, but also undamaged ones.

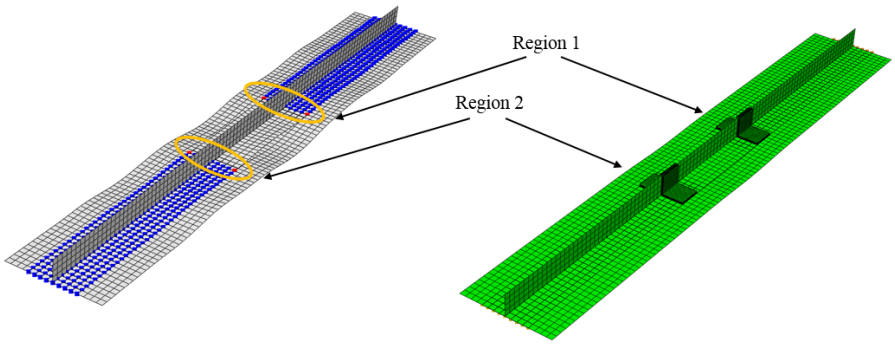

Figure 14: Coupling loop 1. Critical global areas (left) and overlay plot of two corresponding local models (right) for debonded panel D1.

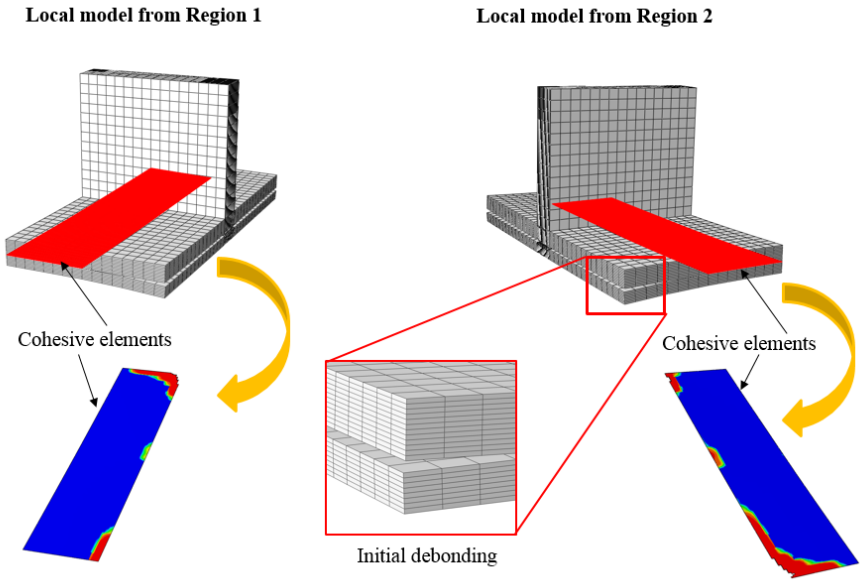

Figure 15: Coupling loop 1. Local models for Regions 1 and 2 with corresponding cohesive elements.

The damage starts from the preliminary debonded areas and propagates further along the pre-debonded edge before growing in the longitudinal directions. The obtained damage evolution path fully corresponds to the experimental results reported in [31]. The full debonded length in global-local analysis increased from 80 mm to 120 mm. As it was reported in [31], the debonding attained the value of 165 mm, though it was also stated that the fibre fracture could interact with debonding in this case and may influence the difference at the final loads.

Load-displacement curves are shown in Fig. 16 for global-local coupling results compared to experimental results. Each of the coupling loops has a slight drop-off that corresponds to the reduction of the interface stiffness in the global model after application of new properties from the local models. Comparison to the full solid reference model has been also carried out until a prescribed displacement 1.5 mm, demonstrating a good agreement with the global-local analysis curve. The structural stiffness is regarded as well predicted by global-

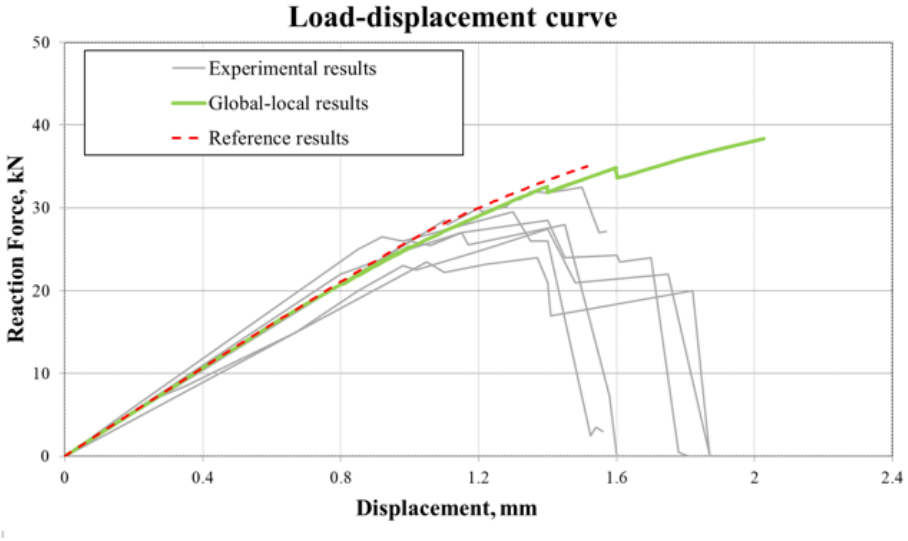

Figure 16: Load-displacement curves of global-local analysis for debonded panel D1 with comparison to experimental results.

local analysis, though since no intralaminar damage was considered, the final collapse could not be attained. That is why the procedure was finished after the prescribed load of 2.0 mm. It is important to note that the global-local approach provides an accurate prediction of the structural behaviour during onset and evolution of the debonding in terms of damage location and stiffness reduction.

5. Conclusion

A novel two-way coupling global-local finite element approach for skin-stringer separation of stiffened composite panels has been developed. The method is based on different levels of accuracy and separate, subsequent simulations of global and local models that is computationally more efficient than full 3D analysis. A global numerical analysis with a standard mesh is performed to define critical areas prone to debonding. Local models are created based on the locations determined by the global analysis. The key challenge of establishing a link between the two models with different discretization level has been

achieved. An accurate information exchange between the global and the local level is ensured by application of discrete and continuum interface elements that follow the same traction-separation law.

Firstly, progressive failure analysis was assessed through the application to the representative case of a one-stringer panel, which demonstrated the effectiveness of the method. Load-displacement curves of the coupling analysis and the solid element reference analysis were in reasonably good agreement. The predictions of both the maximum load level and the sequence of stiffness reductions in the structure showed similar results.

The applicability of the global-local approach was also validated through a comparison with results of a T-stringer panel with an initial debond, previously tested experimentally in [36]. Reasonably good agreement between coupling analysis and experimental results has been demonstrated until the final collapse. As expected, damage started in the area of the initial debonding and propagated further, leading to an increase of skin-stringer separation. However, the smaller regions of debonding predicted in the numerical simulations might be related to the damage modes considered. Intralaminar damage (matrix and fibre damage) were not accounted for in the analyses presented.

The global-local approach developed shows the possibility to establish an effective and efficient procedure for the modelling of skin-stiffener debonding in stiffened composite panels. This global-local technique can be combined with procedures for interlaminar and intralaminar damage of laminates to model the progressive failure of composite panels considering various failure modes.

6. Acknowledgments

The research leading to these results has received funding from European Union's Horizon 2020 research and innovation program (FULLCOMP/2015-2019) under Marie Sklodowska-Curie actions grant agreement number 642121. The provided financial support is gratefully acknowledged by the authors.

[1] R. Degenhardt, A. Kling, H. Klein, W. Hillger, H. C. Goetting, R. Zimmer-

mann, K. Rohwer, Experiments on buckling and postbuckling of thin-walled CFRP structures using advanced measurement systems, International Journal of Structural Stability and Dynamics 7 (2) (2007) 337–358.

[2] R. Krueger, The virtual crack closure technique for modeling interlaminar failure and delamination in advanced composite materials, Elsevier Ltd., 2015. doi:10.1016/B978-0-08-100332-9.00001-3.

[3] E. Rybicki, M.F. Kanninen, A finite element calculation of stress intensity factors by modified crack closure integral, Engineering Fracture Mechanics 9 (1977) 931–938. doi:doi.org/10.1016/0013-7944(77)90013-3.

[4] D. S. Dugdale, Yielding of steel sheets containing slits, J. Mech. Phys. Solids 8 (1960) 100–104.

[5] G. I. Barenblatt, The mathematical theory of equilibrium cracks in brittle fracture, Advances in Applied Mechanics 7 (C) (1962) 55–129. arXiv: S0065-2156(08)70121-2, doi:10.1016/S0065-2156(08)70121-2.

[6] A. Hillerborg, M. Modeer, P.-E. Petersson, Analysis of crack formation and crack growth in concrete by means of fracture mechanics and finite elements, Cement and concrete research 6 (1976) 773–782.

[7] C. Davila, P. Camanho, M. de Mora, Mixed-mode decohesion elements for analyses of proressive delamination, American Institute of Aeronautics and Astronautics (2001) AIAA–01–1486doi:10.2514/6.2001-1486.

[8] A. Turon, P. P. Camanho, J. Costa, An engineering solution for mesh size effects in the simulation of delamination using cohesive zone models, Engineering Fracture Mechanics 74 (2007) 1665–1682. doi:10.1016/j.engfracmech.2006.08.025.

[9] O. Allix, P. Ladevèze, Interlaminar interface modelling for the prediction of laminate delamination, Composite Structures 22 (1992) 235–242.

[10] W.-G. Jiang, S. R. Hallett, B. G. Green, M. R. Wisnom, A concise interface constitutive law for analysis of delamination and splitting in composite materials and its application to scaled notched tensile specimens, International Journal for Numerical Methods in Engineering 69 (9) (2007) 1982–1995. doi:10.1002/nme.1842.
URL http://doi.wiley.com/10.1002/nme.1842

[11] A. Turon, P. P. Camanho, A damage model for the simulation of delamination in advanced composites under variable-mode loading, Mechanics of Materials 38 (2006) 1072–1089. doi:10.1016/j.mechmat.2005.10.003.

[12] P. P. Camanho, C. G. Dávila, Mixed-Mode Decohesion Finite Elements for the Simulation of Delamination in Composite Materials, NASA/TM-2002-211737 (2002) 1–37.

[13] R. Borg, L. Nilsson, K. Simonsson, Simulation of delamination in fiber composites with a discrete cohesive failure model, Composites Science and Technology 61 (5) (2001) 667–677. doi:10.1016/S0266-3538(00)00245-1.

[14] M. R. Wisnom, F. K. Chang, Modelling of splitting and delamination in notched cross-ply laminates, Composites Science and Technology 60 (15) (2000) 2849–2856. doi:10.1016/S0266-3538(00)00170-6.

[15] D. Xie, A. M. Waas, Discrete cohesive zone model for mixed-mode fracture using finite element analysis, Engineering Fracture Mechanics 73 (13) (2006) 1783–1796. doi:10.1016/j.engfracmech.2006.03.006.

[16] S. R. Hallett, M. R. Wisnom, Numerical Investigation of Progressive Damage and the Effect of Layup in Notched Tensile Tests, Journal of Composite Materials 40 (14) (2006) 1229–1245. doi:10.1177/0021998305057432.

[17] J. T. S. Wang, S. B. Bigger, Skin-stiffener interface stresses in composite stiffened panels, NASA Contractor Report 172261.

[18] C. Balzani, W. Wagner, Numerical treatment of damage propagation in axially compressed composite airframe panels, International Journal of Structural Stability and Dynamics 10 (4) (2010) 683–703. doi:10.1142/S0219455410003683.

[19] A. Riccio, A. Raimondo, F. Scaramuzzino, A robust numerical approach for the simulation of skinstringer debonding growth in stiffened composite panels under compression, Composites Part B 71 (2015) 131–142. doi:10.1016/j.compositesb.2014.11.007.

[20] A. Raimondo, A. Riccio, Inter-laminar and intra-laminar damage evolution in composite panels with skin-stringer debonding under compression, Composites Part B 94 (2016) 139–151. doi:10.1016/j.compositesb.2016.03.058.

[21] J. W. H. Yap, M. L. Scott, R. S. Thomson, D. Hachenberg, The analysis of skin-to-stiffener debonding in composite aerospace structures, Composite Structures 57 (1-4) (2002) 425–435. doi:10.1016/S0263-8223(02)00110-1.

[22] B. G. Falzon, G. A. O. Davies, E. Greenhalgh, Failure of thick-skinned stiffener runout sections loaded in uniaxial compression, Composite Structures 53 (2001) 223–233.

[23] S. Hühne, J. Reinoso, E. Jansen, R. Rolfes, A two-way loose coupling procedure for investigating the buckling and damage behaviour of stiffened composite panels, Composite Structures (136) (2016) 513–525. doi:10.1016/j.compstruct.2015.09.056.

[24] R. Krueger, J. G. Ratcliffe, P. J. Minguet, Panel stiffener debonding analysis using a shell / 3D modeling technique, Composites Science and Technology 69 (14) (2009) 2352–2362. doi:10.1016/j.compscitech.2008.12.015.

[25] R. Borrelli, A. Riccio, A. Sellitto, F. Caputo, T. Ludwig, On the use of global local kinematic coupling approaches for delamination growth simulation in stiffened composite panels, Composites Scienece and Technology 115 (2015) 43–51. doi:10.1016/j.compscitech.2015.04.010.

[26] H. Alesi, V. Nguyen, N. Mileshkin, R. Jones, Global/local postbuckling failure analysis of composite stringer/skin panels, AIAA Journal 36 (9). doi:10.2514/2.575.

[27] A. Faggiani, B. G. Falzon, Optimization Strategy for Minimizing Damage in Postbuckling Stiffened Panels, AIAA Journal 45 (10) (2007) 2520–2528. doi:10.2514/1.26910.

[28] J. Bertolini, B. Castanié, J.-j. Barrau, J.-p. Navarro, C. Petiot, Multi-level experimental and numerical analysis of composite stiffener debonding . Part 2 : Element and panel level, Composite Structures 90 (4) (2009) 392–403. doi:10.1016/j.compstruct.2009.04.002.

[29] J. Reinoso, A. Blázquez, A. Estefani, F. París, J. Cañas, E. Arévalo, F. Cruz, Composites : Part B Experimental and three-dimensional global-local finite element analysis of a composite component including degradation process at the interfaces, Composites Part B 43 (4) (2012) 1929–1942. doi:10.1016/j.compositesb.2012.02.010.

[30] R. Vescovini, C. G. Dávila, C. Bisagni, Composites : Part B Failure analysis of composite multi-stringer panels using simplified models, Composites Part B 45 (1) (2013) 939–951. doi:10.1016/j.compositesb.2012.07.030.

[31] A. C. Orifici, I. O. de Zarate Alberdi, R. S. Thomson, J. Bayandor, Compression and post-buckling damage growth and collapse analysis of flat composite stiffened panels, Composites Science and Technology 68 (15-16) (2008) 3150–3160. doi:10.1016/j.compscitech.2008.07.017.

[32] O. Bettinotti, O. Allix, U. Perego, V. Oancea, B. Malherbe, Simulation of delamination under impact using a globallocal method in explicit dynamics,

Finite Elements in Analysis and Design 125 (June 2016) (2017) 1–13. doi:10.1016/j.finel.2016.11.002.

[33] M. Akterskaia, E. Jansen, S. Hühne, R. Rolfes, Efficient progressive failure analysis of multi-stringer stiffened composite panels through a two-way loose coupling global-local approach, Composite Structures 183 (2018) 137–145. doi:10.1016/j.compstruct.2017.02.011.

[34] Abaqus, Abaqus Documentation, Abaqus 6.14 Documentation. Dassault systemes. 6.14 edn. (V) (2017) 1–172.

[35] M. L. Benzeggagh, M. Kenane, Measurement of Mixed-Mode Delamination Fracture Toughness of Unidirectional Glass / Epoxy Composites With Mixed-Mode Bending Apparatus, Composites Science and Technology 56 (1996) 439–449.

[36] A. C. Orifici, R. S. Thomson, R. Degenhardt, A. Kling, K. Rohwer, J. Bayandor, Degradation investigation in a postbuckling composite stiffened fuselage panel, Composite Structures 82 (2008) 217–224. doi:10.1016/j.compstruct.2007.01.012.